Thermography reveals the potential of traditional bean varieties against common bacterial blight

Karina Kazue Nakamura Fukuji

karyna-kazue@hotmail.com

UENF: Universidade Estadual do Norte Fluminense Darcy Ribeiro https://orcid.org/0000-0002-1468-180X

Anderson Yusei Suzuki Fukuji
Cláudia Pombo Sudré
Thâmara Figueiredo Menezes Cavalcanti
Rosana Rodrigues

Research Article

Keywords: Phaseolus vulgaris L., Xanthomonas phaseoli pv. phaseoli, high-precision phenotyping, genetic resistance, infrared thermography

Posted Date: July 14th, 2025

DOI: https://doi.org/10.21203/rs.3.rs-7013874/v1

Abstract

The common bean (*Phaseolus vulgaris* L.) is of great socioeconomic importance in Brazil, being widely cultivated by family farmers who preserve traditional varieties adapted to regional conditions. These varieties represent a strategic source of genetic variability for breeding programs. Among the main phytosanitary obstacles to cultivation, common bacterial blight (CBB), caused by *Xanthomonas phaseoli* pv. *phaseoli* stands out as it compromises bean productivity. This study aimed to evaluate 54 traditional genotypes for resistance to CBC, using visual severity scales and infrared thermography as a complementary tool. The experiment was carried out in a greenhouse, in a randomized block design with three replicates, in two seasons (May and October 2019). Inoculation was performed by two methods (cutting with scissors at 10^7 CFU·mL^{-1} and infiltration with a syringe at 10^6 CFU·mL^{-1}) with the strain Xpp '139-y'. The variables analyzed included area under the disease progress curve (AUDPC), incubation period (IP), and final score (FS). Thermal images were obtained up to three days after inoculation, allowing the calculation of the mean temperature difference (MTD) between healthy and infected tissues. Thermographic analysis enabled early detection of infection, before the appearance of visual symptoms, distinguishing resistant genotypes such as BAC-6 and UENF 2599. The results highlight the potential of thermography as a fast, accurate, and non-destructive method for selecting resistant genotypes, contributing to the modernization and sustainability of bean breeding programs.

INTRODUCTION

Early detection of plant pathogens is essential for maintaining crop health and promoting sustainable phytosanitary management strategies. Although conventional methods, such as diagrammatic scales and lesion measurements, are widely used, they require skilled labor, are time-consuming, and are subject to subjective interpretations (Acco et al. 2020).

In this scenario, innovative technological tools have emerged for their ability to deliver rapid, accurate, and non-invasive diagnoses. Among these, infrared thermography stands out as a promising technique. By converting the infrared emission of plants into visual images, it can reveal physiological changes before visible symptoms appear. This technology enables the detection of abnormal thermal variations associated with metabolic imbalances, supporting preventive and targeted phytosanitary interventions (Pineda et al. 2021; Ban et al. 2025; Agarwal et al. 2025).

During infection, plants often activate defense mechanisms such as stomatal closure, which reduces transpiration and, consequently, increases leaf temperature. These thermal changes can be detected by infrared cameras, facilitating the early identification of infectious processes (Chelladurai and Sujatha 2024). Infrared thermography has proven effective for early disease detection in various crops, establishing itself as a valuable tool for phenotyping pathogen resistance (Hashim et al. 2020; Rippa et al. 2023; Tripathi and Purohit 2025).

In agriculture especially in family-based systems the vulnerability of crops to pathogens and climatic variations poses a significant challenge to production stability. In Brazil, family farming accounts for approximately 69.6% of national bean production (Carvalho et al. 2022), highlighting the need to integrate innovative technologies that can enhance productivity and resilience. Local varieties cultivated by family farmers and traditional communities are noteworthy for their hardiness and natural resistance to pests and diseases, making them fundamental for agrobiodiversity conservation and food security (Brazil 2003; Silva et al. 2025).

Climate change has intensified the occurrence of resistant pests, reduced pollinator activity, and led to soil degradation, underscoring the importance of modern breeding techniques and precise tools for selecting genotypes adapted to these new conditions (Hougue and Breon 2022; Kumar et al. 2020). Among phytosanitary challenges, common bacterial blight (CBC) caused by *Xanthomonas phaseoli* pv. *phaseoli* stands out as a severe disease affecting beans. Typical symptoms include water-soaked leaf spots, which develop into necrotic lesions surrounded by a yellow halo. The disease can also affect stems and pods, reducing photosynthetic area, causing premature leaf drop, and leading to significant yield losses (Chen et al. 2021). Therefore, early detection methods such as infrared thermography are crucial for identifying promising genotypes and supporting breeding and improvement programs (Steinhauser 2016).

Given this context, we hypothesize that infrared thermography is an effective tool for the early detection of common bacterial blight in traditional bean genotypes. Thus, the objectives of this study were to (i) assess the potential of infrared thermography for

early detection of CBC in beans, and (ii) identify resistant genotypes to support breeding programs targeting family-based agriculture.

The integrated adoption of these approaches can accelerate the development of more adapted and robust cultivars, promoting the sustainability of family farming and ensuring greater production stability in the face of climate uncertainties.

MATERIAL AND METHODS

Location, Germplasm, and Experimental Conditions

The experiment was carried out at the Research Support Unit of Universidade Estadual do Norte Fluminense Darcy Ribeiro (UENF), in a greenhouse environment. Fifty-four traditional bean genotypes (*Phaseolus vulgaris* L.) from the state of Rio de Janeiro were evaluated, one of which, genotype BAC-6, was used as a control resistant to CBC, caused by the bacterium *X. phaseoli* pv. *phaseoli* (Rodrigues et al. 1999).

The trials were conducted in two distinct periods, May and October 2019, to evaluate the seasonal influence on the responses of the genotypes. In the first trial, concentrations of 10^6(1) and 10^7(1) were used, with the concentration of 10^6(1) being used to evaluate disease severity and thermography. In the second trial, concentrations of 10^6(2) and 10^7(2) were used. The experimental design used was randomized blocks (DBC), with three replicates. The experimental units consisted of two plants in pot with a capacity of 5 liters, each containing one plant, filled with a substrate composed of soil and sand a 2:1 ratio.

The environmental conditions inside the greenhouse were monitored throughout the experimental period. In the first season (May), the average temperature ranged from 20°C to 45°C, while in the second season (October), the temperature ranged from 20°C to 40°C.

Preparation of the inoculum

The bacterial isolate *X. phaseoli* pv. *phaseoli* (Xpp 139-y), belonging to the collection of the Plant Genetic Improvement Laboratory (LMGV) of UENF, was used. The colonies were grown on DYGS (Dextrose Yeast Glucose Sucrose) solid culture medium and incubated in a BOD chamber at 26°C for 36 hours, according to the methodology described by Rodrigues Neto et al. (1986), Trindade et al. (2015), Fukuji et al. (2025).

After the incubation period, the colonies were suspended in autoclaved deionized water and the bacterial concentration was adjusted to 10^7 CFU·mL^{-1} using a spectrophotometer. The suspension at a concentration of 10^6 CFU·mL^{-1} was obtained by serial dilution using the same autoclaved deionized water solution.

Bacterial inoculation on leaves

Inoculation was performed during the V3-V4 vegetative stage. Two trifoliate leaves from each plant were inoculated, one by the infiltration method using a hypodermic needle syringe (10^6 CFU·mL^{-1}) (Fukuji et al. 2024) and the other by the scissor cut method (10^7 CFU·mL^{-1}) (Trindade et al. 2015). The negative controls consisted of the application of autoclaved deionized water, using the same methods (infiltration and cutting).

Inoculation and Pathogenicity Test

Visual evaluations by the scissor cutting method were performed daily for 18 days after inoculation, with a concentration of 10^7 CFU·mL^{-1}. 1: Highly resistant (no apparent lesion); 2: Resistant (1 to 5% necrosis); 3: Moderately resistant (6 to 25% necrosis); 4: Susceptible (26 to 50% necrosis) and 5: Highly susceptible (> 51% necrosis) (Pastor-Corrales 1981).

Visual assessments using the syringe infiltration method were performed daily for six days, with a concentration of 10^6 CFU·mL^{-1}. The severity of CBC was quantified based on scales described by Fukuji et al. (2025), 1: Highly resistant (no apparent lesion); 2: resistant (presence of chlorotic lesion); 3: moderately resistant (presence of chlorotic lesion with necrotic spots); 4: susceptible (necrotic lesions with chlorotic halo) and 5: highly susceptible (necrotic lesion with chlorotic halo).

Thermographic analyses were conducted exclusively in the first trial, using the syringe infiltration method (10^6 CFU·mL^{-1}).

The quantification of disease progression in the leaves was performed by calculating the Area Under the Disease Progress Curve (AUDPC), according to Shaner and Finney (1977).

Analysis of thermal images

Thermal images were obtained in the first experiment, performed at three time points: 24, 48, and 72 hours after inoculation (1, 2, and 3 days after inoculation – DAI). The leaves of the bean genotypes, inoculated by the infiltration method with the bacterial suspension of Xpp at a concentration of 10^6 CFU·mL^{-1}, were captured with a FLIR T450sc (Forward Looking Infrared) thermal imaging camera.

The images were captured at approximately 30 cm from the leaves, at times of peak solar radiation (between 11:30 a.m. and 2:00 p.m.), on days with clear skies and no cloud cover, to minimize environmental interference (Gomez, 2014).

The images were analyzed using FLIR Tools software (FLIR Systems AB, Danderyd, Sweden), using the Rainbow and Rainbow HC palettes to optimize the thermal contrast between healthy tissues and damaged areas. Temperature measurements were taken at two specific points on the same leaflet: -inoculated area: region infiltrated with the bacterial suspension; -non-inoculated area: region of the same leaflet, visually healthy, used as an internal control (Fig. 1).

The Mean temperature difference (MTD) was calculated as the difference between the average temperature of the inoculated area and that of the non-inoculated area on the same leaf using the equation: $MTD = T_{Fi} - T_{Fn}$

Where: T_{Fi}: Average temperature (°C) of the leaf area inoculated with Xpp; T_{Fn}: Average temperature (°C) of the non-inoculated leaf area (control).

Analysis of CBC Severity Data

The disease severity data on the leaves were analyzed using model 21 of the Selegen-REML/BLUP software, the deviance analysis was constructed according to Viana and Resende (2014), and the LRT (likelihood ratio test) was used to test the effects.

CBC severity variables and thermography

Spearman's nonparametric correlation analyses (1904) were performed to compare the variables MTD 24h, MTD 48h, and MTD 72h, in addition to AUDPC, PI, and FS in the leaves by the two inoculation/concentration methods (infiltration 10^6 CFU.mL^{-1} and scissor cut 10^7 CFU.mL^{-1}) conducted in two trials. Principal Component Analysis (PCA) with clusters and Heatmap were performed to evaluate the influence of resistance and temperature variables on genotypes. All statistical analyses were performed using Selegen-REML/BLUP and R software with packages corrplot, heatmap, ggplot2, MultivariateAnalysis and factoextra.

RESULTS

The AUDPC variable had a significant effect in all experiments, indicating that genotypes differ in disease progression over time (Table 1). The FS variable was highly significant in both experiments. In experiment 10^7(2), FS presented an LRT of 149.00 ($p < 0.01$). The concentrations 10^7 and 10^6 CFU·mL^{-1} impacted the genotypes' response to infection, with 10^7 associated with faster disease development, while 10^6 CFU·mL^{-1} allowed for better differentiation between genotypes.

Table 1

Deviance analysis for the two trials at inoculation concentrations of 10^6 CFU·mL^{-1} inoculated by syringe infiltration and 10^7 CFU·mL^{-1} inoculated by the scissor cut method, for the variables AUDPC, PI, and FS.

	10^6(1)					
	AUDPC		PI		FS	
Effect	Deviance	LRT (x2)	Deviance	LRT (x2)	Deviance	LRT (x2)
Genotypes	524.08	13.41**	153.72	1.89ns	137.68	21.75**
Full Model	537.49		155.61		159.43	
	10^6(2)					
	AUDPC		IP		FS	
Effect	Deviance	LRT (x2)	Deviance	LRT (x2)	Deviance	LRT (x2)
Genotypes	975.14	6.84**	602.06	0.61ns	310.27	11.37**
Full Model	981.98		602.67		321.64	
	10^7(1)					
	AUDPC		PI		FS	
Effect	Deviance	LRT (x2)	Deviance	LRT (x2)	Deviance	LRT (x2)
Genotypes	884.37	28.82**	471.97	50.99**	188.85	36.42**
Full Model	913.19		522.96		225.27	
	10^7(2)					
	AUDPC		PI		FS	
Effect	Deviance	LRT (x2)	Deviance	LRT (x2)	Deviance	LRT (x2)
Genotypes	1314.28	66.05**	651.82	31.09**	24.39	149**
Full Model	1380.33		682.92		173.39	

AUDPC: area under the disease progress curve; IP: incubation period; FS: final score.

Heredity in the broad sense (h^2g) varied among the traits evaluated. Using the classification proposed by Resende (1995), low heritability (0.01–0.15) was observed for AUDPC and IP under certain conditions, reflecting a strong environmental influence. In contrast, variables such as final score (FS) showed moderate to high heritability (0.15–0.50 and > 0.50, respectively), suggesting strong genetic control and good prospects for selection (Table 2). The variation in heritability between seasons, especially notable for IP (0.03 to 0.57), emphasizes the importance of considering genotype–environment interaction in selection. The heritability of the mean of the lines (h^2mg) showed moderate to high values, being particularly high for FS in one of the experimental conditions (0.89), evidencing its robustness as a selective criterion.

Genetic variance (Vg) reflected marked genetic differences, particularly for AUDPC in experiments with 10^7 CFU·mL^{-1} inoculation, indicating high genetic influence on resistance expression. FS showed consistent genetic variance values, reinforcing its stability as a criterion. On the other hand, IP showed lower genetic variability, highlighting its greater susceptibility to external environmental factors.

The expected genetic gain was high for AUDPC and FS, especially under inoculation of 10^7 CFU·mL^{-1}, reflecting that selection based on these variables can generate significant advances in resistance. Selective accuracy, which measures the quality of information for genetic selection (Resende, 2002), was very high for FS and AUDPC under specific conditions (0.94 and 0.88),

ensuring reliability in the identification of superior genotypes. According to Resende & Duarte (2007), only IP in concentration 10^6(2) showed low accuracy, suggesting caution when using this parameter.

A significant negative correlation was observed between IP and AUDPC, indicating that the longer the incubation period, the lower the accumulation of the disease over time (Fig. 2A). This behavior was evident both at a concentration of 10^6 (r = -0.81 in Test 1 and r = -0.79 in Test 2) and at 10^7 (r = -0.73 in Test 1 and r = -0.58 in Test 2) (Fig. 2A). Similarly, a high positive correlation was observed between AUDPC and the final score, ranging from 0.86 (10^6(1)) to 0.91 (10^7(1)), confirming that the greater the severity accumulated over time, the greater the final expression of the disease.

Table 2
Genetic parameters of pathogenicity variables for resistance to *Xanthomonas phaseoli pv. phaseoli* using the syringe infiltration inoculation method at a concentration of 10^6 CFU·mL^{-1} and the scissor cut inoculation method at a concentration of 10^7 CFU·mL^{-1} for both tests.

	10^6(1)			10^6(2)			10^7(1)			10^7(2)		
Genetic Parameters	AUDPC	IP	FS	AUDPC	IP	FS	AUDPC	IP	FS	AUDPC	IP	FS
Vg	2.67	0.10	0.34	1.58	0.11	0.18	47.51	5.30	0.70	24.18	1.21	0.41
Ve	6.22	0.78	0.56	11.22	3.05	0.94	58.98	3.85	0.71	32.58	3.07	0.24
Vf	8.89	0.88	0.90	12.80	3.16	1.12	106.49	9.15	1.41	56.76	4.28	0.65
h^2g	0.30	0.11	0.38	0.12	0.03	0.16	0.45	0.58	0.50	0.43	0.28	0.64
h^2mg	0.56	0.27	0.65	0.41	0.15	0.49	0.71	0.81	0.75	0.79	0.66	0.90
Ac	0.75	0.52	0.81	0.64	0.39	0.70	0.84	0.90	0.87	0.89	0.81	0.95
CVgi%	12.05	12.10	13.44	10.79	11.74	14.66	16.06	30.15	21.09	11.99	11.84	15.13
CVe%	18.40	34.41	17.08	28.72	61.98	33.26	17.90	25.70	21.18	13.92	18.87	11.45
Overall mean	13.55	2.57	4.36	11.66	2.82	2.91	42.92	7.64	3.97	41.02	9.29	4.25

Vg: genotypic variance; Ve: residual (environmental) variance; Vf: phenotypic variance; h^2g: heritability in the broad sense at the plot level, i.e., of genotypic effects; h^2mg: heritability of the mean of genotypes; Ac: selective accuracy; CVgi%: genotypic coefficient of variation; CVe%: residual coefficient of variation; overall mean of the experiment.

The relationship between IP and FS was also consistently negative (–0.73 in 10^6 (1) and – 0.70 in 10^7 (1)), suggesting that materials with greater resistance (represented by higher IP) tend to have lower final scores, demonstrating lower severity. The inoculum concentration exerted a direct influence on the correlation patterns observed. At the lowest concentration (10^6 CFU·mL^{-1}), more extreme correlations were observed, both negative and positive. The correlation between AUDPC and IP at 10^6(1) was the most negative in the study (–0.81), indicating that the delay in infection strongly impacts disease progression when the pathogen is present in low quantities.

The most robust correlations between trials occurred for the FS variable, which showed a correlation of 0.66 between trials at a concentration of 10^7, indicating that the final score of the disease is a relatively stable parameter when evaluated under high inoculum pressure.

The heatmap generated from the multivariate analysis allowed visualization of consistent clusters among genotypes, reflecting their phenotypic responses to the pathogen. The separation of the most resistant genotypes from the most susceptible ones was clearly highlighted. The BAC-6 and UENF 2599 genotypes formed a group characterized by high IP values (reddish tones) and low FS and AUDPC values (dark blue tones) (Fig. 2B), which shows low severity and effective containment of disease progression over time.

Principal component analysis (PCA), combined with cluster grouping, provided a comprehensive view of the variability of the genotypes evaluated for parameters related to disease resistance. The first two principal components together explained 72.12% of the total data variability, with 55.7% attributed to the first component (PC1) and 16.42% to the second component (PC2) (Fig. 3).

Three distinct groups were formed: Group 1 (red): Comprises the genotypes located in the lower right and upper right quadrants of the biplot. These materials correlate directly with the IP variables of the most aggressive isolates 10^7(1) IP, 10^7(2) IP, 10^6(1) IP, and 10^6(2) IP, which have vectors directed in the same orientation. This behavior indicates that the genotypes in this group have intermediate incubation period values, favoring faster disease development. Genotypes such as UENF 2349, UENF 2350, UENF 2376, UENF 2391, UENF 2595, UENF 2598, and UENF 2590, among others, are included in this group, consistent with intermediate materials for resistance to Xpp. Group 2 (green): Represented by genotypes BAC-6 and UENF 2599, located in isolation in the upper right quadrant, they are markedly distant from the others, indicating a high degree of resistance. This group has a strong association with the IP vector. This positioning demonstrates that these genotypes have high IP values and low severity, reflected by low FS and AUDPC values. Group 3 (blue): Positioned mainly in the lower and upper left quadrants, this group brings together susceptible genotypes, evidenced by their moderate negative association with IP vectors and positive association with FS and AUDPC vectors.

The correlation analysis between the epidemiological indicators of CBC severity and the mean temperature difference (MTD) obtained by thermography revealed significant associations, which reinforce the usefulness of this technique for early detection of the disease (Figure 4).

The MTD showed moderate to strong correlations with AUDPC (r = 0.68 and r = 0.72, respectively) and FS (r = 0.71 and r = 0.67). These results indicate that greater thermal differences between infected and uninfected tissue are associated with increased disease severity, suggesting that MTD is sensitive to physiological changes induced by infection (Fig. 5A). In addition, the negative correlation between IP and MTD (r = -0.54 at 48 h and r = − 0.52 at 72 h) confirms that resistant genotypes, with longer incubation times, show less thermal variation in the early stages of infection. The lower MTD values observed in resistant genotypes indicate a lower physiological impact from infection, reflecting the ability of these materials to maintain a more stable thermal balance, even under biotic stress.

The multivariate analysis represented in the heatmap enabled the integrated visualization of physiological and epidemiological data of bean genotypes against Xpp infection, under inoculation by syringe infiltration at a concentration of 10^6 CFU·mL^{-1}. Hierarchical clustering showed the formation of two contrasting groups of genotypes. At the bottom of the dendrogram, genotypes BAC-6 (resistant control) and UENF 2599 stood out, both with high IP values and low FS and AUDPC values, visually represented by bluish tones. In addition, these genotypes showed low thermal variation (MTD) over the 72 hours, indicating a stable physiological response to infection (Fig. 5B).

In contrast, genotypes located at the upper end of the dendrogram, such as UENF 2575, UENF 2348, and UENF 2374, showed low resistance, characterized by the lowest IP value (blue tones), high FS and AUDPC values, and high MTD, especially at 48 and 72 hours after inoculation, evidenced by intense red coloration. These data indicate more accelerated disease progression, greater leaf temperature change, and low efficiency of defense mechanisms against bacterial infection.

Among the variables evaluated, MTD at 48h and 72h was especially informative for discriminating phenotypic groups, with a correlation pattern consistent with the other epidemiological indicators of resistance. Genotypes with higher MTD in the early stages of infection also showed greater severity, as observed for AUDPC and FS, while resistant genotypes maintained more homogeneous temperatures, even under pathogen pressure.

Principal component analysis (PCA) was effective in discriminating the genotypes evaluated for resistance to the Xpp pathogen. Principal component 1 (PC1) was strongly associated with variables related to disease severity, such as AUDPC, FS, and MTD at 24, 48, and 72 hours, which showed a negative correlation with the IP variable. Thus, genotypes positioned in the left quadrant of the biplot showed greater severity, accelerated disease progression, and shorter incubation periods, while those positioned on the right were characterized by greater resistance, reflected by longer IP, lower AUDPC and FS values, and smaller MTD variations in the different time windows.

The formation of three distinct groups was observed, representing different levels of resistance of the genotypes (Fig. 6). Group 1 (represented in red) grouped the genotypes considered highly susceptible, which presented the lowest IP values and the highest AUDPC, FS, and MTD values (24h, 48h, and 72h). Group 2 (represented in green) comprised genotypes with intermediate resistance, characterized by average IP, AUDPC, FS, and MTD values. Finally, Group 3 (represented in blue) included genotypes with a high level of resistance, clearly standing out from the others. This group includes genotypes BAC-6 (resistant control), UENF 2599, UENF 2351, UENF 2387, UENF 2305, and UENF 2353, which showed prolonged IP, low AUDPC and FS values, and significant reductions in MTD over the three days of evaluation (24h, 48h, and 72h). The clear separation of this group in the biplot reflects the presence of efficient resistance mechanisms capable of delaying the onset of symptoms and reducing the severity of the disease over time. The presence of the resistant control BAC-6 in this group validates the criteria used for grouping and confirms the robustness of the method applied.

DISCUSSION

The significant effect of the AUDPC variable demonstrates that disease progression varies among genotypes, which is a determining factor in the evaluation of resistance. The high significance of the FS variable, especially in experiment 10^7(2), highlights its importance as a parameter for resistance assessment. Additionally, the inoculum concentration influenced the results: the higher concentration (10^7 CFU·mL^{-1}) led to more rapid disease development, whereas the lower concentration (10^6 CFU·mL^{-1}) provided greater resolution for distinguishing between genotypes, reinforcing its utility for phenotyping resistance.

The results indicate that heritability in the broad sense varies among the evaluated traits, with AUDPC and IP being more influenced by environmental conditions, while FS is under stronger genetic control and offers better prospects for selection. The observed seasonal variation, particularly for IP, underscores the importance of considering genotype–environment interactions in breeding programs. The high heritability of the mean of the lines, especially for FS, highlights its potential as a robust selection criterion.

Genetic variance data further support the relevance of AUDPC and FS as reliable indicators for resistance selection, as both showed marked genetic differences and stability across conditions. In contrast, the lower genetic variability of IP suggests that it is more susceptible to environmental fluctuations, reducing its usefulness as a direct selection parameter.

The high expected genetic gain for AUDPC and FS under high inoculum concentration (10^7 CFU·mL^{-1}) indicates that selection for these traits can effectively advance resistance breeding. The very high selective accuracy for FS and AUDPC under specific conditions ensures confidence in identifying superior genotypes, while the low accuracy observed for IP under certain conditions reinforces the need for caution when relying on this variable.

The identification of a significant negative correlation between IP and AUDPC supports the conclusion that delayed symptom onset contributes to slower disease progression, in agreement with previous studies (Castrillon et al. 2020). The strong positive correlation between AUDPC and final score validates the use of FS as a practical and efficient indicator of disease severity at the end of the trials, particularly when continuous assessments are impractical (Trindade et al. 2015; Fukuji et al. 2024). These findings reinforce the value of AUDPC and FS as key criteria for selecting resistance to X. phaseoli pv. phaseoli, whereas the greater environmental influence on IP limits its reliability for direct selection. As highlighted by Vencovsky and Barriga (1992), the estimation of genetic parameters is highly dependent on specific experimental conditions, and caution is needed when comparing results across studies.

The strong dependence of inoculum pressure on the relationships between epidemiological variables highlights the need to use multiple inoculum levels in breeding programs to ensure the selection of resistant materials under both low and high disease pressure conditions. The more extreme correlations observed at the lowest inoculum concentration suggest that, under lower disease pressure, there is a greater expression of genetic differences among the evaluated materials, in agreement with Nechet and Halfeld-Vieira (2011).

The positioning of UENF 2599 alongside BAC-6, a known resistant control, reinforces that this genotype has highly efficient resistance mechanisms, both in prolonging the incubation period and in containing disease development (low FS and AUDPC). This finding validates the superior performance of the UENF 2599 genotype and suggests that its response may be related to

mechanisms such as phytoalexin production, activation of pathogenesis-related proteins (PR), and the generation of reactive oxygen species (ROS), which are typical in resistant plants and contribute to limiting infection (Kaur et al., 2022). Additionally, Fukuji et al. (2025) identified 48 candidate genes related to CBB resistance, including those involved in defense responses, jasmonic acid pathways, receptor-like kinase (RLK) proteins, and other disease resistance-related proteins. The observation that quantitative resistance plays a key role reinforces its importance as a sustainable approach, reducing selective pressure on the pathogen and enhancing the durability of resistant cultivars, as suggested by Viteri et al. (2014).

The results from PCA and cluster analysis further support the conclusion that there is considerable variability among genotypes for resistance-related parameters, and that the first two principal components capture the majority of this variation, facilitating the identification of genotypes with desirable resistance traits.

The results obtained corroborate the robustness of the multivariate analyses applied, both in the separation of genetic groups and in the interpretation of the resistance of the materials to the disease. The formation of a cluster exclusively by BAC-6 and UENF 2599 is especially relevant, since it confirms that UENF 2599 has resistance equivalent to the standard control, demonstrating its potential to be used in breeding programs.

The observed correlations between MTD and both AUDPC and FS highlight the potential of thermal imaging as a sensitive indicator of disease severity in beans infected by Xpp. The negative correlation between IP and MTD reinforces the notion that resistant genotypes are capable of delaying symptom onset and maintaining lower thermal variation during early infection, supporting the use of thermography as an early screening tool in resistance breeding.

The identification of BAC-6 and UENF 2599 as resistant genotypes, based on both physiological (MTD) and epidemiological parameters (IP, FS, and AUDPC), reinforces the robustness of these materials for breeding programs. Their stable thermal profiles under infection further underline their ability to tolerate biotic stress, likely due to more effective or rapid activation of defense mechanisms. Conversely, the more susceptible genotypes exhibited greater thermal instability and more severe disease progression, which may be associated with a lower efficiency in mounting defense responses after pathogen challenge.

The results obtained by multivariate analysis not only confirm the value of integrating physiological and epidemiological data for a comprehensive assessment of resistance, but also validate the practical application of thermography in discriminating between resistant and susceptible genotypes in early stages of infection.

These results confirm the applicability of thermography as a complementary tool in resistance phenotyping, allowing early detection of physiological changes associated with infection, even before the visible manifestation of symptoms. The consistency observed between thermal data and traditional severity parameters reinforces the potential of the integrated use of these approaches to increase the accuracy and efficiency of genetic improvement programs aimed at resistance to common bacterial blight.

These findings are in line with previous studies. For example, Vagelas et al. (2021) demonstrated the effectiveness of infrared thermography for the presymptomatic detection of leaf diseases in grapevine, chrysanthemum, and rose. Rippa et al. (2023) showed that infrared thermography was effective in the early detection of rot caused by Rhizoctonia solani and Sclerotinia sclerotiorum in arugula, with diseases being identified 3 to 6 days before visible wilting. Additionally, Rippa et al. (2024) demonstrated the effectiveness of thermography for detecting Fusarium oxysporum f. sp. raphani infections in wild arugula at an early stage, between 30 and 48 hours after inoculation.

The results are also consistent with previous studies showing that resistant genotypes not only have lower severity but also more balanced physiological responses to bacterial infection. The UENF 2599 genotype showed superior performance, comparable to the BAC-6 control, which highlights its potential as a source of resistance in genetic improvement programs.

Overall, the multivariate analysis presented here allowed for the efficient classification of genotypes in terms of resistance to common bacterial blight, demonstrating the importance of the integrated use of epidemiological (AUDPC, FS, and IP) and physiological (MTD) variables in the selection of superior materials.

CONCLUSIONS

The results demonstrate the effectiveness of thermography as an accurate tool for early detection and evaluation of resistance to CBB in bean genotypes. The BAC-6 and UENF 2599 genotypes stood out for having longer IP, lower FS, lower AUDPC, and reduced MTD differential at 24h, 48h, and 72h after inoculation.

Thus, this study shows that thermography enables the early and efficient identification of promising materials, contributing significantly to the optimization of genetic improvement programs aimed at resistance to phytopathogens.

Declarations

Acknowledgements Conselho Nacional de Desenvolvimento Científico e Tecnológico (CNPq), Fundação Carlos Chagas Filho de Amparo à Pesquisa do Estado do Rio de Janeiro (FAPERJ), Coordenação de Aperfeiçoamento de Pessoal de Nível Superior—Brasil (CAPES)—Finance Code 001.

Authors' contribution KKNF, AYSF conceived and designed the research, KKNF, CPS, AYSF designed methodology, KKNF, AYSF, CPS, TFMC, RR validated the manuscript, KKNF, AYSF performed data analysis, KKNF, AYSF, CPS, RR reviewed and edited the manuscript. All authors have read and agreed to the published version of the manuscript.

Funding This study was financed by the Coordenação de Aperfeiçoamento de Pessoal de Nível Superior—Brasil (CAPES)—Finance Code 001, Fundação Carlos Chagas Filho de Amparo à Pesquisa do Estado do Rio de Janeiro (FAPERJ) and Conselho Nacional de Desenvolvimento Científico e Tecnológico (CNPq). The first author received research fellowship from the CAPES.

Data availability The datasets generated during and/or analysed during the current study are available from the corresponding author on reasonable request.

Conflict of interest The authors declare no competing interests.

References

1. Acco LF, Gomes DG, Matos JN, Ribeiro NR, Balbi-Peña MI (2020) Development and validation of a diagrammatic scale for evaluating bacterial pustule in soybeans. Summa Phytopathol. 46:145–149. Available online: https://doi.org/10.1590/0100-5405/211476 (accessed on 20 Apr 2025).
2. Agarwal A, Colwell FdJ, Dinnis R, Galvis VC, Hill TR, Boonham N, Prashar A (2025) Infrared thermography in plant factories: solving spatiotemporal variations via machine learning. Mod. Agric. 3:10.
3. Ban S, Tian M, Hu D, Xu M, Yuan T, Zheng X, Li L, Wei S (2025) Evaluation and early detection of downy mildew of lettuce using hyperspectral imagery. Agriculture 15:444. Available online: https://doi.org/10.3390/agriculture15050444 (accessed on 18 Jan 2025).
4. Fukuji KKN, Fukuji AYS, Gonçalves LSA, Delfini J, Cirino VM, Rodrigues R (2025) Association mapping of bean reaction to common bacterial blight by SNP markers. Bragantia 84:e20240120. Available online: https://doi.org/10.1590/1678-4499.20240120 (accessed on 02 Mar 2025).
5. Pineda M, Barón M, Pérez-Bueno ML (2021) Thermal imaging for plant stress detection and phenotyping. Remote Sens. 13:68.
6. Castrillon MAdSC, Barelli MAA, Corrêa CL, Pereira SVdS, Almici M, Vendruscolo TPS, Silva RSS, Zago BW, Duarte AVM, Silva DD, Araújo KL, Viana L, Tardin FD (2020) Multivariate analysis of resistance components of the saccharin and biomass sorghum to Ramulispora sorghi. Sci. Electron. Arch. 13:39. Available online: https://doi.org/10.36560/13520201027 (accessed on 05 Feb 2025).
7. Chelladurai K, Sujatha N (2024) A review of leaf disease detection using thermal camera-based image processing techniques. Int. J. Intell. Syst. Appl. Eng. 12(10s):175–184.
8. Chen NWG, Ruh M, Darrasse A, Foucher J, Briand M, Costa J, Studholme DJ, Jacques MA (2021) Common bacterial blight of beans: a model of seed transmission and pathological convergence. Mol. Plant Pathol. 22(12):1464–1480.
9. Gomez S (2014) Infection and spread of Peronospora sparsa on Rosa sp. (Berk.): a microscopic and thermographic approach. Dissertation, University of Bonn, Germany.

10. Hashim IC, Shariff ARM, Bejo SK, Muharam FM, Ahmad K, Hashim H (2020) Application of thermal imaging for plant disease detection. IOP Conf. Ser. Earth Environ. Sci. 540:012052. Available online: https://iopscience.iop.org/article/10.1088/1755-1315/540/1/012052 (accessed on 21 Jan 2025).
11. Hougue AS, Breon K (2022) The biggest threats to species. Conserv. Sci. Pract. e12670:01–09.
12. Kaur S, Samota MK, Choudhary M, Choudhary M, Pandey AK, Sharma A, Thakur J (2022) How do plants defend themselves against pathogens—Biochemical mechanisms and genetic interventions. Physiol. Mol. Biol. Plants 28(2):485–504. Available online: https://doi.org/10.1007/s12298-022-01146-y (accessed on 11 Feb 2025).
13. Kumar S, Pandey G (2020) Biofortification of pulses and legumes to enhance nutrition. Heliyon 6:e04163.
14. Nechet KL, Halfeld-Vieira BA (2011) Effect of inoculum, leaf wetness period and phenological stage of cowpea on honeydew development. Trop. Plant Pathol. 36(2):105–111.
15. Pastor-Corrales MA, Beebe SE, Correa FJ (1981) Comparing two inoculation techniques for evaluating resistance in beans to Xanthomonas campestris pv. phaseoli. In: International Conference on Plant Pathogenic Bacteria. International Center for Tropical Agriculture, Cali, Colombia, p. 493–503.
16. Resende MDV (1995) Design of selection experiments to maximize selective accuracy and genetic progress. Rev. Árvore 19:479–500.
17. Resende MDV, Duarte JB (2007) Precision and quality control in cultivar evaluation experiments. Pesq. Agropecu. Trop. 37:182–194.
18. Resende MDV (2002) Genética biométrica e estatística no melhoramento de plantas perenes. Brasília: Embrapa Informação Tecnológica, 975 p.
19. Rippa M, Pasqualini A, Curcio R, Mormile P, Pane C (2023) Active vs. passive thermal imaging for helping the early detection of soil-borne rot diseases on wild rocket (Diplotaxis tenuifolia). Plants 12:1615. Available online: https://doi.org/10.3390/plants12081615 (accessed on 15 Apr 2025).
20. Rippa M, Pasqualini A, Manganiello G, Woo SL, Mormile P, Pane C (2024) Thermal imaging applications in early disease detection. ACS Agric. Sci. Technol. 4(5):544–553. Available online: https://doi.org/10.1021/acsagscitech.3c00582 (accessed on 23 Jan 2025).
21. Rodrigues Neto J, Malavolta JR, Victor O (1986) Simple medium for the isolation and cultivation of Xanthomonas campestris pv. citri type B. Summa Phytopathol. 12:16.
22. Shaner G, Finney RF (1977) The effects of nitrogen fertilization on the expression of slow-mildewing in Knox wheat. Phytopathology 70:1183–1186.
23. Silva JR, Silva LSN, Santos MF (2025) O patrimônio genético e cultural das sementes crioulas na percepção de discentes da Licenciatura em Educação do Campo de Picos-PI. Rev. Prát. Docência 9.
24. Spearman C (1904) “General Intelligence”, objectively determined and measured. Am. J. Psychol. 15:201–293.
25. Sudré CP (2015) Combining ability for common bacterial blight resistance in snap and dry bean (Phaseolus vulgaris L.). Acta Sci. Agron. 37:37–43.
26. Tripathi V, Purohit A (2025) Thermal imaging and disease detection in Hibiscus plant. Int. J. Res. Appl. Sci. Eng. Technol. 13:4621–4636. Available online: https://doi.org/10.22214/ijraset.2025.69191 (accessed on 08 Apr 2025).
27. Vagelas I, Papadimos A, Lykas C (2021) Pre-symptomatic disease detection in the vine, chrysanthemum, and rose leaves with a low-cost infrared sensor. Agronomy 11:1682.
28. Vencovsky R, Barriga P (1992) Genética biométrica no fitomelhoramento. Ribeirão Preto: Sociedade Brasileira de Genética.
29. Viana AP, Resende MDV (2014) Genética quantitativa no melhoramento de fruteiras. Rio de Janeiro: Interciência, 296 p.
30. Viteri DM, Cregan PB, Trapp JJ, Miklas PN, Singh SP (2014) A new common bacterial blight resistance QTL in Vax 1 common bean and interaction of the new QTL, SAP6, and SU91 with bacterial strains. Crop Sci. 54:1598–1608.

Figures

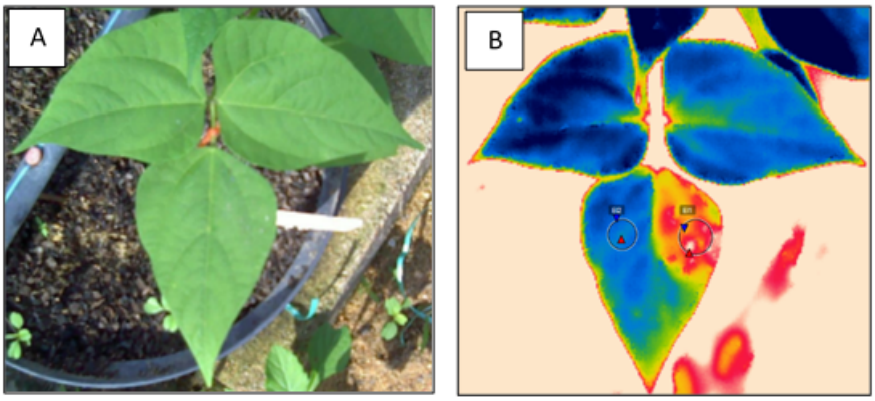

Figure 1

Representation of disease development in bean leaves inoculated by infiltration with *Xanthomonas phaseoli* pv. *phaseoli*. A) Reflection image (RGB) and B) Thermal image with measurement points for leaf area (red, higher temperature) and healthy leaf area (blue, lower temperature).

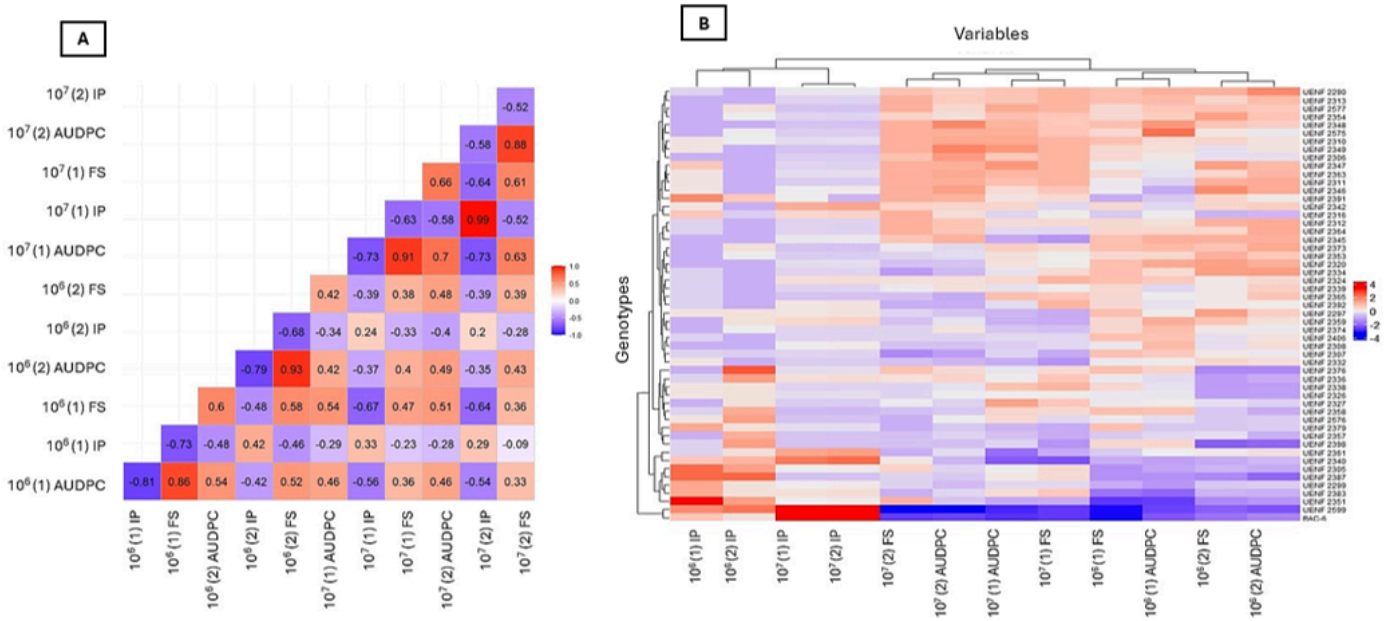

Figure 2

A. Correlation analysis between indicators of severity of *Xanthomonas phaseoli* pv. *phaseoli* in bean plants using the methods of inoculation by syringe infiltration (10^6 CFU·mL^{-1}) and cutting with scissors (10^7 CFU·mL^{-1}) in two experimental trials. Area Under the Disease Progress Curve (AUDPC), Incubation Period (IP) and Final Score (FS) for first (1) and second (2) trials; **B.** Heatmap of severity indices for resistance to *Xanthomonas phaseoli* pv. *phaseoli* in bean genotypes using the syringe infiltration (10^6 CFU·mL^{-1}) and scissor cut (10^7 CFU·mL^{-1}) inoculation methods in two trials. Area Under the Disease Progress Curve (AUDPC), Incubation Period (IP) and Final Score (FS) for first (1) and second (2) trials.

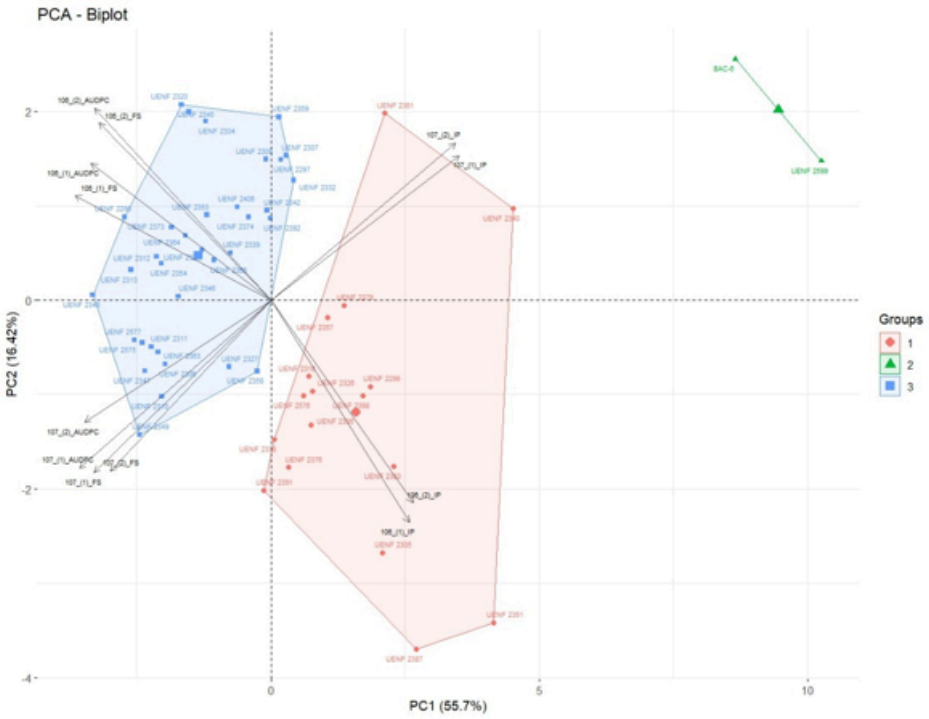

Figure 3

PCA-biplot analysis with cluster grouping based on severity indices for resistance to *Xanthomonas phaseoli* pv. *phaseoli* in bean genotypes evaluated by syringe infiltration (10^6 CFU·mL^{-1}) and scissor cut (10^7 CFU·mL^{-1}) inoculation methods in two trials.

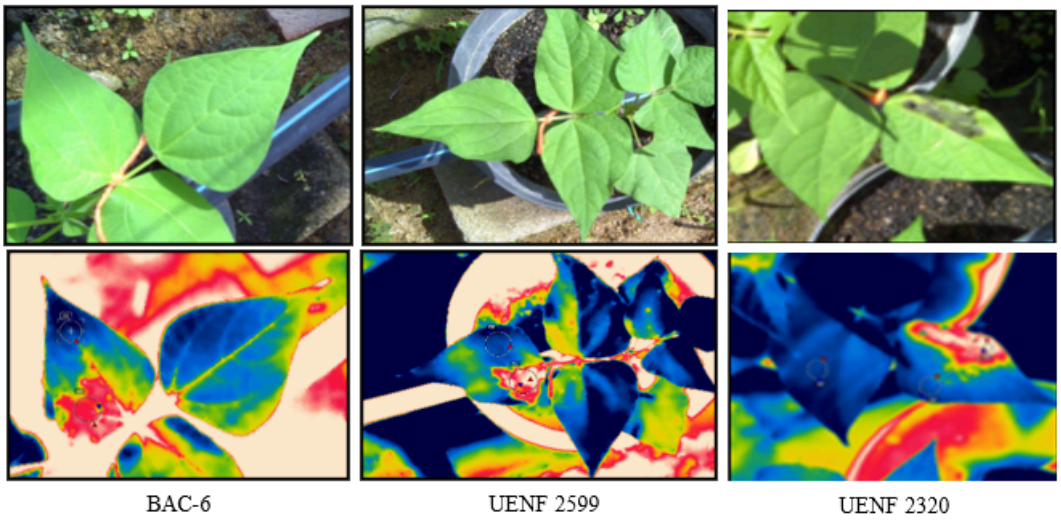

Figure 4

Thermographic images of resistant and susceptible bean genotypes inoculated with *Xanthomonas phaseoli* pv. *phaseoli*, using the syringe infiltration inoculation method at a concentration of 10^6 CFU·mL^{-1}, on the third day of evaluation.

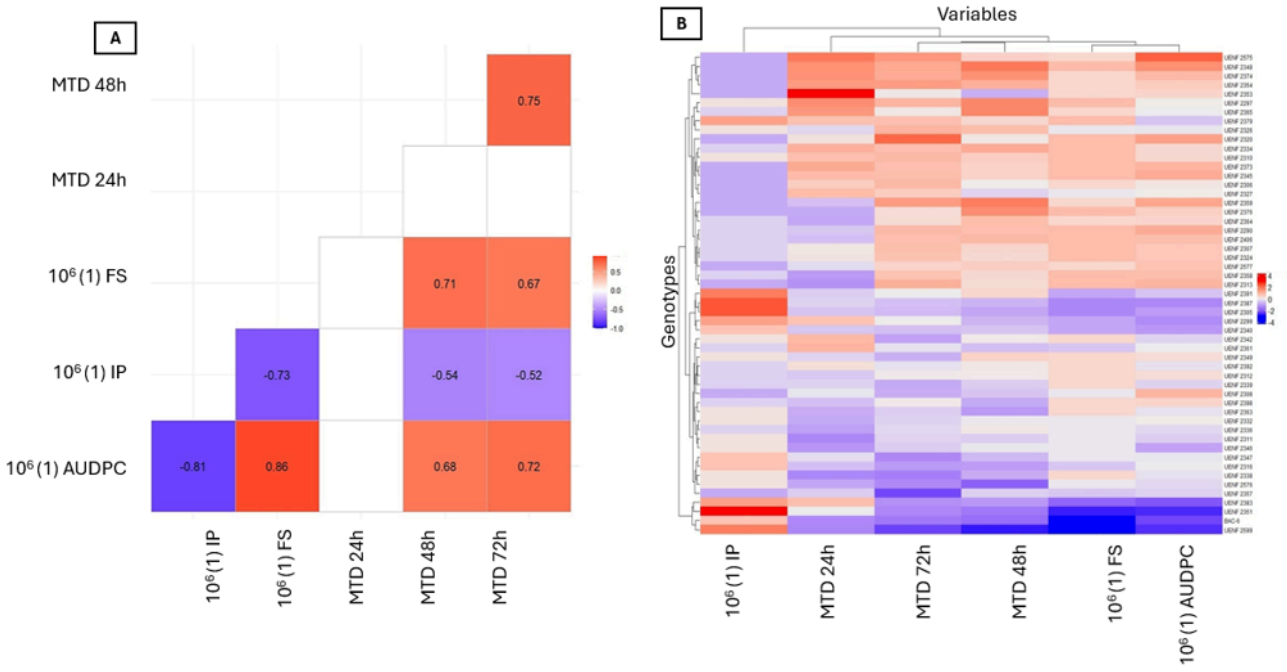

Figure 5

A. Correlation analysis between indicators of severity of *Xanthomonas phaseoli* pv. *phaseoli* in beans and the mean temperature differential in the first three days after inoculation by syringe infiltration (10^6 CFU·mL^{-1}) in trial 1. Area Under the Disease Progress Curve (AUDPC), Incubation Period (IP), Final Score (FS), Mean Temperature Difference (MTD) for first (1) trial. **B.** Heatmap correlation between severity indices of common bacterial blight and the mean temperature differential in bean genotypes inoculated by syringe infiltration (10^6 CFU·mL^{-1}) over three days. Area Under the Disease Progress Curve (AUDPC), Incubation Period (IP) and Final Score (FS) for first (1) trial.

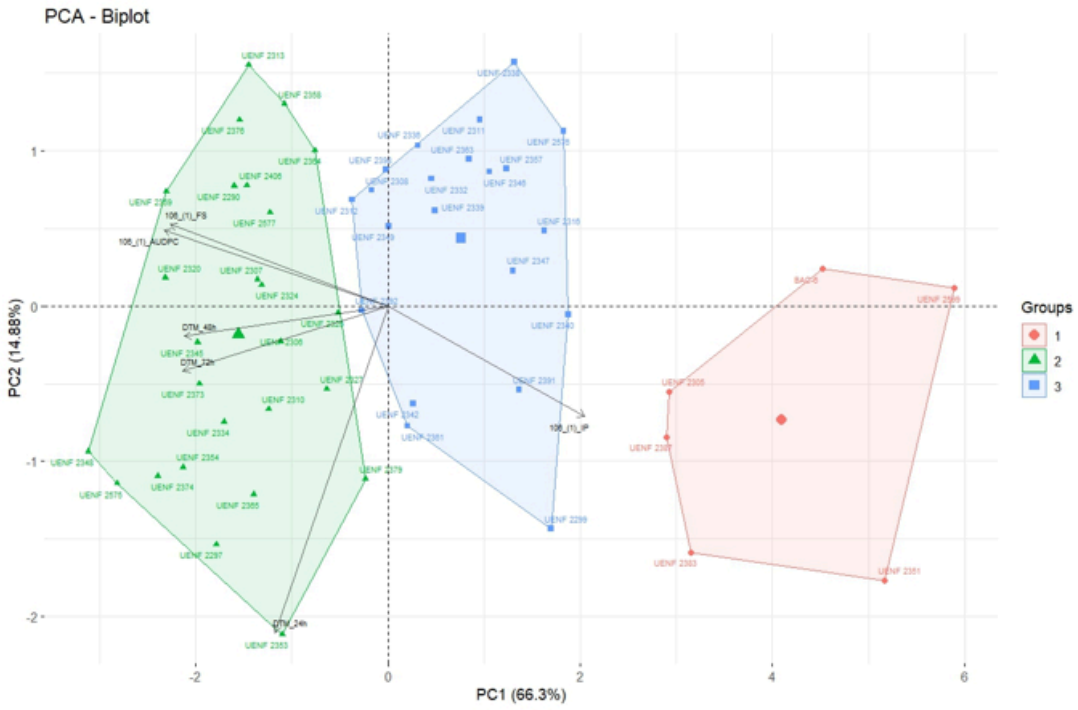

Figure 6

PCA-biplot analysis with cluster grouping in bean genotypes based on common bacterial blight severity indices and mean temperature difference during three days after inoculation by the syringe infiltration method (10^6 CFU·mL^{-1}).